

Comparison of the $\mathbf{k}\cdot\mathbf{p}$ and direct diagonalization approaches to the electronic structure of InAs/GaAs quantum dots

L. W. Wang, A. J. Williamson, and Alex Zunger^{a)}

National Renewable Energy Laboratory, Golden, Colorado 80401

H. Jiang and J. Singh

Department of Electrical Engineering and Computer Science, The University of Michigan, Ann Arbor, Michigan 48109-2122

(Received 13 September 1999; accepted for publication 16 November 1999)

We present a comparison of the 8-band $\mathbf{k}\cdot\mathbf{p}$ and empirical pseudopotential approaches to describing the electronic structure of pyramidal InAs/GaAs self-assembled quantum dots. We find a generally good agreement between the two methods. The most significant shortcomings found in the $\mathbf{k}\cdot\mathbf{p}$ calculation are (i) a reduced splitting of the electron p states (3 vs 24 meV), (ii) an incorrect in-plane polarization ratio for electron-hole dipole transitions (0.97 vs 1.24), and (iii) an over confinement of both electron (48 meV) and hole states (52 meV), resulting in a band gap error of 100 meV. We introduce a ‘‘linear combination of bulk bands’’ technique which produces results similar to a full direct diagonalization pseudopotential calculation, at a cost similar to the $\mathbf{k}\cdot\mathbf{p}$ method. © 2000 American Institute of Physics. [S0003-6951(00)01903-3]

Self-assembled, Stranski–Krastanow (SK) grown semiconductor quantum dots such as InAs/GaAs have recently received considerable attention.¹ They exhibit a rich spectrum of phenomena including quantum confinement, exchange splittings, Coulomb charging/blockade, and multiexciton transitions. However, given that the precise shape, size, inhomogeneous strain and alloying profiles of these dots is difficult to measure, accurate theoretical modeling becomes crucial. Modeling can determine if the predicted electronic structure resulting from the *assumed* shape, size, strain, and alloying profiles agrees with spectroscopic and transport measurements or not. Early calculations used simple single-band effective-mass models,^{2,3} which are assumed^{4,5} to be too crude to describe these effects. More recently, 8-band $\mathbf{k}\cdot\mathbf{p}$ effective-mass models have become available for SK dots^{4–6} and free-standing dots.⁷ In this approach, the states of the dots are determined by expanding them in a basis containing the zone center (Γ) bulk valence band maximum (VBM) states (six states, including spin) and the bulk conduction-band minimum (CBM) (two states, including spin),

$$\Psi_i^{\mathbf{k}\cdot\mathbf{p}}(\mathbf{r}) = \sum_{n=1}^{N_B} f_n^{(i)}(\mathbf{r}) u_{n,\Gamma}(\mathbf{r}). \quad (1)$$

Although $N_B=8$ currently represents the state of the art as far as effective mass, envelope function based methods are concerned, it is of great interest to determine how accurate this approach really is. Unfortunately, agreement with experiment, as important as it is, is not by itself a sufficient test in this case, since the 8-band $\mathbf{k}\cdot\mathbf{p}$ model includes many parameters whose values are not accurately known, but can significantly influence the results.⁸ Furthermore, investigating convergence by systematically increasing the number of

bands, N_B , is mathematically cumbersome. Thus, it is currently unknown if the $N_B=8$ model is converged or not.

However, it is now possible¹ to avoid the effective mass and envelope function approximations and solve for the electronic structure of dots containing $\sim 10^6$ atoms using the same pseudopotential methodology with which ordinary bulk semiconductors were treated so successfully over the past 30 years.⁹ In this pseudopotential approach the wave function, $\psi_i(r)$, is a solution of the following Schrodinger’s equation:

$$\left\{ -\frac{1}{2}\nabla^2 + \sum_{n\alpha} \hat{v}_\alpha(r-R_{n\alpha}) \right\} \psi_i(x) = \epsilon_i \psi_i(x), \quad (2)$$

where $\hat{v}_\alpha(r-R_{n\alpha})$ is the pseudopotential of atomic type α and $R_{n\alpha}$ is the relaxed position of the n th atom of type α . The relaxed atomic positions are determined by minimizing the *atomistic* elastic energy as described by the valence force field (VFF) method.¹⁰ The atomic pseudopotentials $\{v_\alpha\}$ are strain dependent and are carefully fitted¹¹ to the measured bulk band gaps [so that the ‘‘local density approximation (LDA) error’’ does not occur], effective masses and to first-principles calculations of the band offsets¹² and deformation potentials.¹³ The wave functions $\psi(x)$ are expanded in a plane wave basis set. Eigenstates are calculated using a fast diagonalization method¹⁴ (the ‘‘folded spectrum method’’) implemented on massively parallel supercomputers. This direct diagonalization (DD) pseudopotential method has been applied to superlattices,¹⁵ random, and ordered alloys,¹⁶ free-standing (i.e., colloidal) semiconductor dots^{17–19} and self-assembled dots.^{19,20}

An interesting aspect of the DD pseudopotential approach is that its basic equation [Eq. (2)] can be solved for bulk compounds which allows one to determine²¹ the pseudopotential $\mathbf{k}\cdot\mathbf{p}$ parameters. These parameters can then be used as input to a single or 8-band $\mathbf{k}\cdot\mathbf{p}$ calculation for a quantum dot. Given their identical input, a comparison of the DD and $\mathbf{k}\cdot\mathbf{p}$ calculated electronic structures can be used to

^{a)}Electronic mail: azunger@nrel.gov

TABLE I. Properties of the InAs and GaAs pseudopotential band structures at lattice constants of 6.058 and 5.653 Å. Δ is the spin-orbit splitting, and $a_c(\Gamma)$, $a_v(\Gamma)$, b , and d are the deformation potentials. γ_1 , γ_2 , and γ_3 are the conventional Luttinger parameters. E_p is calculated as $2|\langle\psi_n|p_z|\psi_c\rangle|^2$. Note, this empirical pseudopotential method differs from that used in Ref. 20 which did not include the spin-orbit interaction.

Property	InAs	GaAs
E_g (eV)	0.410	1.518
E_{vbm} (eV)	-5.577	-5.622
m_e	0.032	0.092
$m_{hh}, m_{lh}[100]$	0.48, 0.040	0.47, 0.122
Δ (eV)	0.36	0.33
$a_c(\Gamma), a_v(\Gamma)$ (eV)	-4.49, -0.85	-7.63, -1.00
b (eV)	-1.85	-1.77
d (eV)	-3.32	-3.1
$\gamma_1, \gamma_2, \gamma_3$	10.60, 4.37, 4.90	4.76, 1.39, 1.98
E_p (eV)	14.63	16.95

examine differences in the underlying approximations of the methods. Such comparisons between $\mathbf{k}\cdot\mathbf{p}$ and pseudopotentials, using identical bulk inputs have already been performed for bulk solids,²¹ superlattices,²¹ and free-standing quantum dots.^{17,18} The comparisons for free-standing (30–50 Å) InP,¹⁷ CdSe,¹⁸ and InAs¹⁹ dots highlighted several shortcomings of the 8-band $\mathbf{k}\cdot\mathbf{p}$ (e.g., Ref. 7) relative to the potential approach: (i) 8-band $\mathbf{k}\cdot\mathbf{p}$ finds the highest energy hole state to have a p -like symmetry in both InP and InAs, compared to a majority s -like symmetry obtained by DD approach;¹⁷ (ii) the electron states in InP derived from the bulk L point in the Brillouin zone, found in the DD approach¹⁷ are absent in the 8-band $\mathbf{k}\cdot\mathbf{p}$ method; (iii) the strong mixing of states with s and p symmetry, found by the DD method for InAs hole states,¹⁹ are absent in the $\mathbf{k}\cdot\mathbf{p}$ results; (iv) as a result of the exaggerated confinement of hole states about half the hole states found by the DD in CdSe¹⁸ within 300 meV of the VBM are altogether missed by the $\mathbf{k}\cdot\mathbf{p}$ approach; and (v) “intrinsic surface states” recently predicted²² by 8 band $\mathbf{k}\cdot\mathbf{p}$ arise from an unphysical basis set.²³

Here we conduct a comparison of the single ($N_B=1$) and 8-band $\mathbf{k}\cdot\mathbf{p}$ and DD pseudopotential approaches for a pyramidal InAs quantum dot, with a base of 113 Å and a height of 56 Å, embedded within a GaAs barrier. The two approaches use identical bulk inputs (Table I) and an identical strain profile, obtained from an atomistic VFF calculation. One could, of course, have chosen slightly different input parameters, but we believe that as long as one uses the same input to the $\mathbf{k}\cdot\mathbf{p}$ and pseudopotentials, the *difference* between the results will not change significantly. For this larger, embedded quantum dot system we find a much better agreement between the two approaches than was found^{24,18} for the ~30–50 Å diameter free-standing dots.

The single band calculations use a plane wave basis set. The strain modified InAs effective masses are set to $m_e^* = 0.04$, $m_{hh,\parallel}^* = 0.042$, and $m_{hh,\perp}^* = 0.538$. The potential offset profiles were obtained by coupling the VFF strain profile to the deformation potentials in Table I. In the 8-band calculations,⁵ a real space, numerical grid is used to describe the envelope functions and the finite difference method is used to calculate the spatial gradients and Laplacian operators. One grid point is used for each eight atom cubic cell,

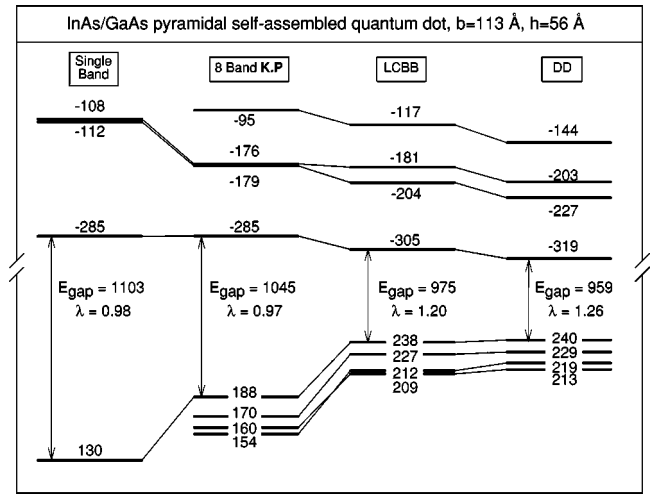


FIG. 1. The energy levels of an InAs/GaAs pyramidal quantum dot with a base of 113 Å and height of 56 Å, calculated using the 1 and 8 band $\mathbf{k}\cdot\mathbf{p}$ and direct diagonalization (DD) empirical pseudopotential method, and the LCBB method. The electron (hole) energies are in meV with respect to the CBM(VBM) of bulk GaAs. λ is the $[110]:[\bar{1}10]$ dipole transition ratio.

which sufficiently converges the final $\mathbf{k}\cdot\mathbf{p}$ result. The energy levels and wave functions obtained by the single and 8-band $\mathbf{k}\cdot\mathbf{p}$ and DD pseudopotential approaches are compared in Figs. 1 and 2.

Electron states: The wave functions of the electron states are very similar. The lowest state is s -like, the next two are the split p states, and the fourth is d -like. The 8-band $\mathbf{k}\cdot\mathbf{p}$ does not capture the elongation of the s and d states along the $[110]$ direction. In the single and 8 band $\mathbf{k}\cdot\mathbf{p}$ the splitting of the p states, is zero⁴ if one uses continuum elasticity to determine the strain profile and is found to still be small (~3 meV) when using our atomistic VFF strain profile. However, in the DD pseudopotential calculation, this splitting is much larger (24 meV). Overall, the single and 8-band $\mathbf{k}\cdot\mathbf{p}$ electron states are too high in energy (over-confined) and the intraband splittings are too large.

Hole states: The hole states cannot be classified as s , p , d , etc. due to the strong interband mixing. With one exception, $\mathbf{k}\cdot\mathbf{p}$ produces hole states with a one–one correspondence to the DD states. However, they are over-confined by 50–70 meV and the intraband splittings are too large by up to 7 meV. The first hole state is perfectly isotropic in the 8-band $\mathbf{k}\cdot\mathbf{p}$ model, while the DD pseudopotential calculation produces a strong anisotropy along the $[110]$ direction. In the single-band calculation, only the first hole state corresponds to the DD state, and this is overconfined by 110 meV.

Electron-hole recombination energy: The single- and 8-band recombination energies (1.103 and 1.045 eV) are 144 and 86 meV higher than that found by DD. The absence of spatial anisotropy in their e_0 and h_0 wave functions, also leads to an error (0.97 and 0.98 vs 1.26) in the polarization ratio, λ , for dipole transitions along the two in-plane directions $[110]$ and $[\bar{1}10]$.

Several attempts have been made to provide simple, ad hoc, corrections to the 8-band $\mathbf{k}\cdot\mathbf{p}$, such as additional interface terms.²⁵ Instead of these ad hoc corrections, we have recently developed²⁶ an alternative Linear Combination of Bulk Bands (LCBB) basis representation which is more approximate than the full DD basis set, but far less computa-

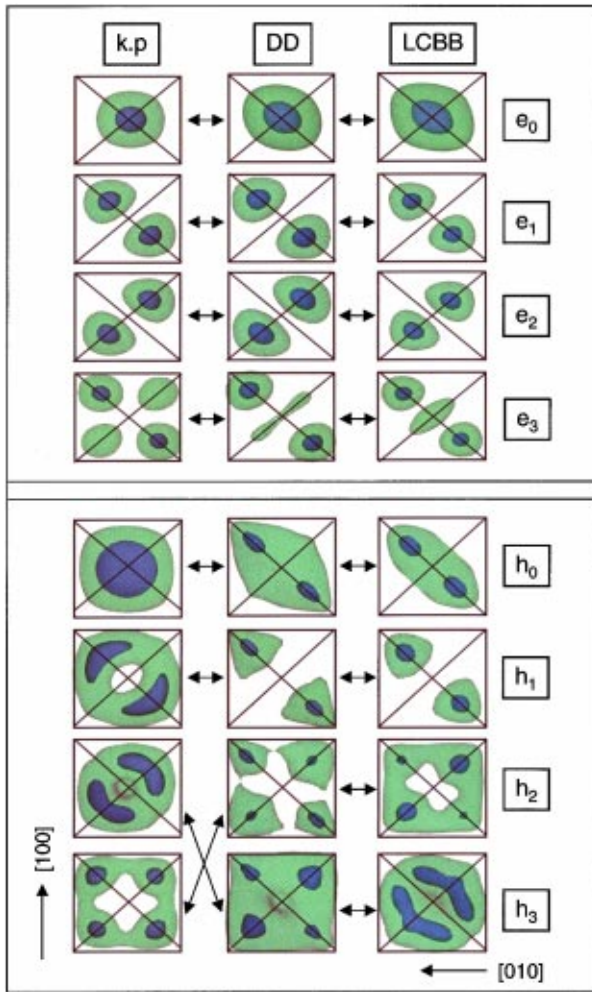


FIG. 2. (Color) Charge density isosurfaces of the electron and hole states. The green and blue isosurfaces represent 25% and 75% of the charge density amplitude.

tionally expensive. In this approach, we do not limit the basis to Γ -like states [Eq. (1)], but also include bulk Bloch functions, computed for a given value, ϵ , of the strain.

$$\Psi_i^{\text{LCBB}}(\mathbf{r}) = \sum_n^{N_B} \sum_k^{N_k} [C_{n,k}^{(i)} e^{i\mathbf{k}\cdot\mathbf{r}}] u_{n,k}(\epsilon, \mathbf{r}), \quad (3)$$

where N_B and N_k are a cutoff for the number of bands and k points. The speed up of the LCBB method compared to the DD pseudopotential method arises from the fact that the LCBB states form a physically more intuitive basis than traditional plane waves and N_B and N_k can be significantly reduced to keep only the physically important bands and k points (around the Γ point in this case). In the wave function

expansion [Eq. (3)] we include bulk Bloch states from (i) bulk InAs and GaAs at zero pressure and (ii) InAs subjected to the strain profile in the center and tip of the dot. We include all k points with $12\pi/L$ of the Γ point, where L is the supercell dimension. Figures 1 and 2 show that the LCBB captures all of the features of the DD pseudopotential approach which distinguish it from the 8-band $\mathbf{k}\cdot\mathbf{p}$. In particular, LCBB gives (i) an eigenvalue error $\sum_{i=1}^4 |\epsilon_{\text{DD}}^i - \epsilon_{\text{LCBB}}^i|$ of only 15 meV for hole states (compared with 229 meV for 8-band $\mathbf{k}\cdot\mathbf{p}$) and 86 meV for electrons (compared to 158 meV for $\mathbf{k}\cdot\mathbf{p}$), (ii) correct wave function anisotropy for the e_0 and h_0 states and consequently a polarization ratio of 1.20, and (iii) the correct p -state splitting of 23 meV. The LCBB is therefore able to capture the main features of the more computationally expensive DD approach at a similar computational cost to the 8-band $\mathbf{k}\cdot\mathbf{p}$ method.

The above results are specific to the InAs/GaAs SK dot system. It is difficult to make predictions for other material combinations, but one might expect the agreement between the effective mass and DD approaches to improve for larger nanostructures, such as InP dots grown on GaP.

This work was supported by DOE—Basic Energy Sciences, Division of Materials Science under Contract No. DE-AC36-98-GO10337.

- ¹A. Zunger, *Mater. Res. Bull.* **23**, 35 (1998).
- ²M. Grundmann, O. Stier, and D. Bimberg, *Phys. Rev. B* **52**, 11969 (1995).
- ³J.-Y. Marzin, J.-M. Gerard, A. Izrael, D. Barrier, and G. Bastard, *Phys. Rev. Lett.* **73**, 716 (1994).
- ⁴C. Pryor, *Phys. Rev. B* **57**, 7190 (1998).
- ⁵H. Jiang and J. Singh, *Appl. Phys. Lett.* **71**, 3239 (1997).
- ⁶O. Stier, M. Grundmann, and D. Bimberg, *Phys. Rev. B* **59**, 5688 (1999).
- ⁷A. Efros and M. Rosen, *Phys. Rev. B* **58**, 7120 (1998).
- ⁸C. Pryor, *Phys. Rev. B* **60**, 2869 (1999).
- ⁹M. L. Cohen and J. Chelikowsky, *Electronic Structure and Optical Properties of Semiconductors* (Springer, Berlin, 1988).
- ¹⁰P. Keating, *Phys. Rev.* **145**, 637 (1966).
- ¹¹T. Mattila, L.-W. Wang, and A. Zunger, *Phys. Rev. B* **59**, 15270 (1999).
- ¹²S.-H. Wei and A. Zunger, *Appl. Phys. Lett.* **72**, 2011 (1998).
- ¹³A. Franceschetti, S.-H. Wei, and A. Zunger, *Phys. Rev. B* **50**, 17797 (1994).
- ¹⁴L.-W. Wang and A. Zunger, *Semiconductor Nanoclusters* (Elsevier Science, Amsterdam, 1996).
- ¹⁵K. Mader, L.-W. Wang, and A. Zunger, *Phys. Rev. Lett.* **74**, 2555 (1995).
- ¹⁶T. Mattila, S.-H. Wei, and A. Zunger, *Phys. Rev. Lett.* **83**, 2010 (1999).
- ¹⁷H. Fu and A. Zunger, *Phys. Rev. Lett.* **80**, 5397 (1998).
- ¹⁸L.-W. Wang and A. Zunger, *J. Phys. Chem.* **102**, 6449 (1998).
- ¹⁹A. Williamson and A. Zunger, *Phys. Rev. B* **59**, 15819 (1999).
- ²⁰J. Kim, L.-W. Wang, and A. Zunger, *Phys. Rev. B* **57**, R9408 (1998).
- ²¹D. Wood and A. Zunger, *Phys. Rev. B* **53**, 7949 (1996).
- ²²P. Sercel, A. Efros, and M. Rosen, *Phys. Rev. Lett.* **83**, 2394 (1999).
- ²³L.-W. Wang, *Phys. Rev. B* (in press).
- ²⁴H. Fu and A. Zunger, *Phys. Rev. B* **57**, R15064 (1998).
- ²⁵B. Foreman, *Phys. Rev. Lett.* **80**, 3823 (1998).
- ²⁶L.-W. Wang and A. Zunger, *Phys. Rev. B* **59**, 15806 (1999).